Design Of Intelligent Low Voltage Load Switch For Remote Control System In Smart Grid

Dezhi Xiong[1], Xiangqun Chen[1] , Radek Martinek[2], He Wen[3,*], Derong Luo[3] and Janusz Smulko[4]

[1] Hunan Province Key Laboratory of Intelligent Electrical Measurement and Application Technology, State Grid Hunan Electric Power Company Power Supply Service Center (Metrology Center), China; dzhxiong@outlook.com, chenxiangqun0@outlook.com

[2] Faculty of Electrical Engineering and Computer Science, VSB - Technical University of Ostrava; radek.martinek@vsb.cz

[3] College of Electrical and information engineering, Hunan University; he_wen82@126.com, hdldr@sina.com

[4] Faculty of Electronics, Telecommunications and Informatics, Gdansk University of Technology; jsmulko@eti.pg.edu.pl

* Correspondence: he_wen82@126.com;

Abstract: Current low-voltage load switches do not support remote disconnect/connect and real-time monitoring of a disconnect/connect state. Addressing to these issues, this paper presents a low voltage load switch for a smart remote control system, which uses a one-chip microcontroller board and a DC step motor drive mechanism and provides the feedback on the switch status also. Arrears disconnect and full-pay connect control is implemented via the microcomputer and Hall sensor. The low-power supply and state feedback circuit are designed to reduce the power consumption. And the motor drive mechanism is optimized to improve the performance of motor. Finally, a test environment includes the system control and feedback is created to illustrate the feasibility of the designed low-voltage switch. The test results that the design supports disconnect/connect control and state feedback in various conditions validate the feasibility of this designed system, which has high practical value and is worthy of promotion.

1. Introduction

In smart grid, electric customers should know and control their electric costs through smart electricity meters, which is helpful for improving the electric system reliability and reducing the carbon emissions in the energy conservation [1]. The embedded switch is widely used in smart electricity meters for the control of the power supply [2-3]. The utilities can also use such an electricity meter with an embedded switch to ensure that customers will pay their electricity charges in a timely manner. Nowadays, the remote control and state detection of the embedded switch are very important because both electric customers and utilities would like to operate it by APPs. Moreover, the power consumption of the embedded switch is getting more and more attention because it affects the stability and safety. Thus, it is important to design an intelligent low voltage (220V AC system) load switch for a remote control system in a smart grid [4-5].

Typically, the low voltage electric power payment control is implemented via an electricity meter embedded relay or external load switch [6-7]. It is reported that a relay-based control switch for the main power supply circuit is a hidden risk, where the power supply line failure is likely to cause relay burnout [8-9]. This is because a relay does not support arc suppression and has limited overcurrent and breaking capability. Moreover, if the relay is integrated in an electricity meter, it is impossible to replace the relay separately, which means the operational cost with such electricity meter embedded relay are high [10-11].

According to statistics from the State Grid Hunan Electric Power Company of China in 2016, 28000 failure reports of electricity meter via the 95598 Customer Hotline were handled. And 60% of

the failure reports are relay failure. Due to space limits in electricity meters, the relay capacity is limited. Currently, an electricity meter embedded relay has a maximum rated current of 60 A [12-14]. However, it cannot satisfy the increasing electricity consumption because residential users are connecting a larger number of electric appliances with an increasing demand on electricity with improvements in living standards [15-19]. Thus, the demand on a payment control switch with large current specifications is becoming urgent.

An useful way for implementing a payment control switch is the use of an external low-voltage load switch. As an electrical protection component, a low-voltage load switch has superior breaking capability. However, most low-voltage load switches do not support remote control. A low-voltage payment control switch is only an implementation of "semi-automatic" payment control, i.e., when a user is in arrears, a low-voltage load switch is in the disconnect operation [20-23]. In practical, when a user pays a fee, a manual connect is required to restore the power supply [24-26]. In this situation, the operational cost and maintenance workload of utilities would thus increase. In addition, the manual operation or connect has a time delay, which deteriorates the experience satisfaction of customers in power consumption.

Moreover, in current power grids, the transmission of the payment control information is one-way flow, i.e., the utilities send a control command or signal to a payment control switch. There is no feedback of the status of the payment control switch, which means no-one knows whether the operation is success or not. When payment control switch execution is abnormal, a system cannot detect these anomalies and automatically correct these anomalies. Therefore, the total reliability of a payment control system cannot be guaranteed.

In summary, the state-of-art low-voltage load switch does not support remote disconnect/connect and accurate feedback of a disconnect/connect state. In order to address the challenge that current implementations of low-voltage load switch, this paper presents an intelligent low-voltage load switch control method, and designs a state feedback system. An arrears disconnect and full-pay connect control plan is introduced, and a low-power consumption power supply and DC motor state monitoring unit are designed. Moreover, the motor drive mechanism of the presented switch is optimized; and a motor control procedure is presented. The test results indicate that the presented switch in this paper supports an automatic remote disconnect/connect operation and actual feedback of a switch state.

2. Control System Operation and Payment Control

2.1 System Operation

As it is introduced in the last section, it is important to monitor the status of the payment control switch. Thus the load switches should be able to send their status to the remote control center. In this paper, the remote control center is set as the power consumption information collection main station in the State Grid Hunan Electric Power Company of China, which is shown in Fig.1. The concentrator is the information router, which takes charge of the information transfer between intelligent electricity meters and the power consumption information collection main station. In such a power consumption information collection main station, the remote control and state monitoring of intelligent load switches are performed. As shown in Fig.1, there are two line, i.e., the control line and the feedback line, connecting the intelligent smart meter and the intelligent low-voltage load switch. The control and feedback plan are as following.

When a disconnect/connect control procedure is executed, the power consumption information collection main station sends a disconnect/connect instruction to a field concentrator via a communication channel, such as a general packet radio system (GPRS). A concentrator forwards a command to a specific intelligent electricity meter via the power line carrier communication. When an electricity meter receives a disconnect/connect instruction, the control terminal high/low level changes and controls the low-voltage load switch to execute the disconnect/connect command.

The intelligent electricity meters monitor the status of intelligent low-voltage load switches, including the output line voltage by the feedback line and the actual disconnect/connect state of the

switch. The power consumption information collection main station supports real-time monitoring of the field low-voltage load switch disconnect/connect state.
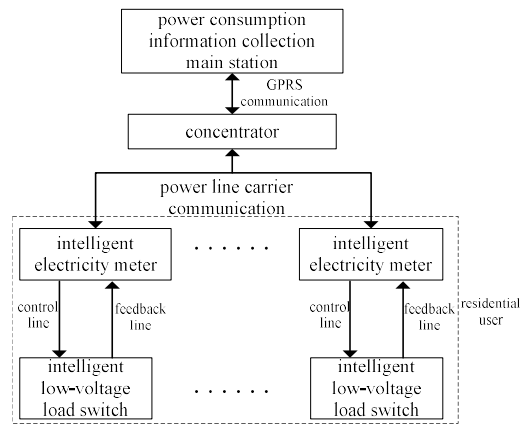

Figure.1   Control and feedback plan in a power consumption information collection main station

2.2   Switch payment control

2.2.1 Arrears disconnect control

In this part, we introduce the design of the intelligent low-voltage load switch in detail. The mechanical part of the intelligent low-voltage load switch is a small low-voltage load switch with superior breaking capability, stable tripping protection and high reliability. As shown in Fig.1, the control instructions from the intelligent electricity meter are transferred by to intelligent low-voltage load switch by the control line. The control part of the intelligent low-voltage load switch is shown in Fig.2. When a low-voltage load switch receives an arrears signal, a multipoint control unit (MCU) generates a disconnect instruction. The motor drives a functional gear to rotate clock-wisely before the trip bar is rotated clock-wisely by the cam in the functional gear. The low-voltage load switch tripping apparatus is lifted. And the low-voltage load switch instantaneously trips. At this moment, the functional gear continues clockwise rotation until the functional gear magnet coincides with the disconnect Hall sensor OH137 [27] on the circuit board. The Hall sensor generates a pulse signal and sends it to a single-chip microcomputer. A stop command will be generated by single-chip microcomputer. As a result, the functional gear stops rotation and locks a tripping mechanism to prevent the low-voltage load switch from manually connecting in an arrears state. The arrears tripping operation is completed.
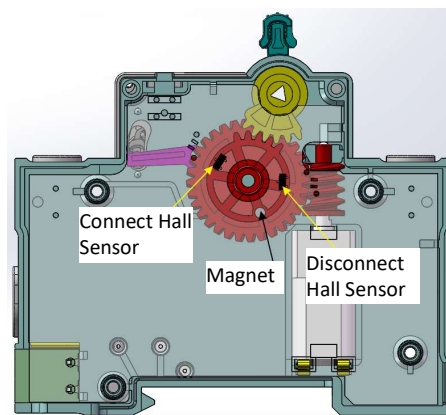

Figure.2   Control part of the intelligent low-voltage load switch

2.2.2 Full-pay connect control

When the low-voltage load switch receives a full-pay signal, the single-chip microcomputer generates an instruction which makes the motor drives the functional gear to rotate clock-wisely. The functional gear releases the tripping shaft, which is in a free state and releases the low-voltage load switch. So the functional gear continues clockwise rotation. The functional gear semi-gear drives the linkage gear rotation. During the connect operation, the linkage gear drives the handle of the switch via the handle linkage rod. The functional gear magnet coincides with the disconnect Hall sensor in the circuit board. A stop command will be generated by the single-chip microcomputer after receiving the pulse signal from the Hall sensor. Thus, the functional gear stops rotation.

3. Load switch control unit

3.1 Principle of control unit

In this part, we presents the detailed design of load switch control unit, which includes modular, software platform and hardware architecture. The system architecture is shown in Fig. 3. The low-power consumption R5F10268 chip with 8k FLASH [28] is adopted as a management microcontroller unit (MCU). The MCU is main control unit of the system that provides the following functions: the control direction switch between the standby power supply and the main power supply, the detection and execution of the electricity meter control signal, the detection of the control switch manual/automatic mode, the execution of the corresponding program, the detection of if a line is disconnected, the detection of the switch state and provide feedback, the control of DC motor operation, the control of infrared electron tube emission and receiving to monitor the motor rotation state. For the automatic disconnect/connect, the position or status of disconnect/connect can be detected by the Hall sensor, which is driven by a direct current (DC) step motor.
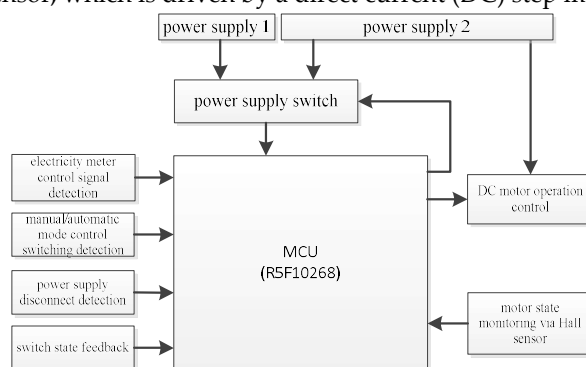

Figure.3   Scheme of the control unit design principle

In Fig.3, the power supply 1 is the standby power supply while power supply 2 is the main power supply which is based on a micro-power switch-mode power supply module. The standby power supply is based on a low-power consumption circuit, whose output current is less than 1 m.. The power supply of the intelligent low-voltage load switch is controlled by an intelligent electricity meter. The power supply 2 provides a power for DC motor operation.

3.2 Low-power consumption power supply and state feedback circuit

In the normal electricity consumption mode, the power supply 2 receive power from control signal line K, which is in a standby state or driving state. The input current of the control signal line of the intelligent low-voltage load switch is an alternating current (AC) less than 1 mA. In a standby state, the output DC voltage of the standby power supply 1 is less than 15 V and the output DC current is less than 0.5 mA. In a driving state, the minimum instantaneous output DC current from standby power supply 1 is 20 mA, where the minimum duration is 20 ms. And the maximum voltage during this period is 8 V.

The real-time output voltage of the load switch is monitored, which is also provided as a feedback to the electricity meter. A semi-wave rectification to charge energy storage capacitors is used in the power supply circuit. When an energy storage capacitor is charged to a certain voltage level, a short period of discharge closes the main power supply control relay. The main power supply locks the control relay to recharge the energy storage capacitor and drives the DC motor operation via MCU control. The state feedback circuit is powered by the load switch lower terminal voltage and connected to a large series resistor for current limiting to ensure operator's safety. The detailed circuit design of the low-power consumption power supply and state feedback is shown in Fig. 4.
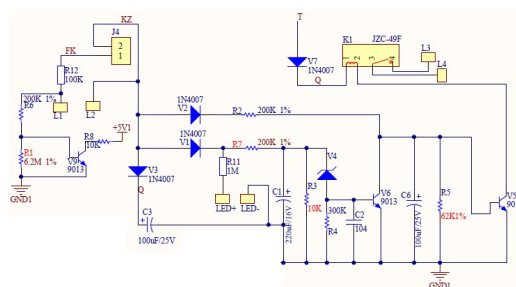

Figure.4 Low-power consumption power supply and state feedback circuit

J4 is the connector for the control line KZ and the feedback line FK. In normal usage, the KZ line AC 220V power supply undergoes semi-wave rectification through V1, V2 and V3 diodes and charges the energy storage capacitors C1, C3 and C6. LED+ and LED- are LED indicator terminals that reflect the capacitor charge status. When the MCU receives or generates a control command, diode V7 is turned on to create a loop. Energy storage capacitors C1, C3 and C6 discharge for a short period of time to drive the close of the main power supply JZC-49F control relay K1. Charged terminal L3 and terminal L4 are turned on to provide power supply for the motor driver circuit. In this manner, the DC motor driver power supply is under control. The main power supply operates and controls relay K1 in a lock state; the terminal L2 power supply is turned on to charge the energy storage capacitor.

L1 is the lower terminal of the low-voltage load switch. After it connects to a series 100 KΩ resistor, the J4 terminal directly provides level signal feedback to the electricity meter, which can be used to monitor the load switch on/off state. When the external load switch is in a connect state, the feedback level is AC 220 V. When the external load switch is in a disconnect state, the feedback terminal has no level signal.

4. The design of motor drive

4.1 Motor drive mechanism design

The motor drive mechanism includes the worm shaft, primary dual bevel gear, secondary dual gear, third dual gear and partial gear. The partial gear and primary dual bevel gear transmission ratio is 419.3. The motor drive mechanism is shown in Fig. 5.
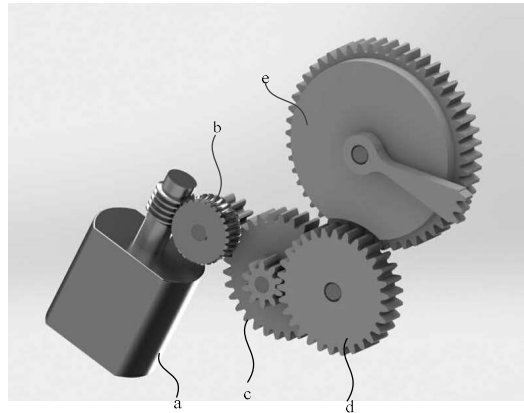
Figure.5   Motor drive mechanism

In the diagram, primary dual bevel gear b meshes with motor drive axial worm shaft a; primary dual bevel gear b meshes with secondary dual gear c; secondary dual gear c meshes with third dual gear d; and third dual gear d meshes with partial gear e.

The gear parameters of the proposed intelligent low-voltage load switch are listed in Table 1.

Table 1.   Parameters of each part

Part	Number of teeth and modulus
number of worm shafts (modulus)	1(0.4 mm)
primary dual bevel gear	26(13)/0.4 mm
secondary dual gear	37(12)/0.4 mm (0.5 mm)
third dual gear	28(14)/0.5 mm (0.6 mm)
partial gear	22/0.6 mm

In Table 1, the numbers in and outside the brackets represent the number of teeth and the modulus of the small and larger gear in the dual bevel gear or dual gear, respectively.

The gear transmission ratio can be calculated from Table 1 as following:

$$I = \frac{26 \times 37 \times 28 \times 34}{12 \times 13 \times 14} = 419.3 \tag{1}$$

Assume that the minimum efficiency of the primary dual bevel gear, secondary dual gear, third dual gear and partial gear in normal usage are 0.4, 0.75, 0.75 and 0.75, respectively. The radius of the disconnect/connect rod (not shown in the diagram) is 15 mm. Thus, the final level of the idle torque under load is expressed as following:

$$T_2 = 419.3 \times 1.43 \times 0.4 \times 0.75 \times 0.75 \times 0.75 = 101.2N \tag{2}$$

The connect state damping torque is T_3, and the connect state motor torque under load is T_5. The following relation holds:

$$T_2 - T_3 = 419.3 \times T_5 \times 0.4 \times 0.75 \times 0.75 \times 0.75 \tag{3}$$

Based on equation (3), the motor torque under load T_5 can be calculated as

$$T_5 = 9550 \times P / n_5 \tag{4}$$

where n_5 is the motor rotation speed under load, P is the motor power (kW).

Based on equation (5), the disconnect/connect state rod angular velocity is ω_1:

$$\omega_1 = n_5 / I \tag{5}$$

Accordingly, the connect operation time t_1 can be obtained.

The disconnect state motor torque under load T_6 can be calculated as following:

$$T_2 + T_4 = 419.3 \times T_6 \times 0.4 \times 0.75 \times 0.75 \times 0.75 \tag{6}$$

where T_4 is the disconnect state slave force, which is unknown.

Based on equation (7), the motor on-load rotation speed n_6 is expressed as follow:

$$n_6 = 9550 \times P / T_6 \tag{7}$$

Then, the disconnect state angular velocity ω_2 is expressed as follow:

$$\omega_2 = n_6 / I \tag{8}$$

Based on the angular velocity ω_2, the disconnect operation time t_2 can be calculated.

Assume the disconnect/connect rod rotation angle is θ_1, and the partial gear rotation angle is θ_2. When disconnect or connect is completed, the partial gear is rotated back the angle θ_3 to facilitate the next operation and leave space for manual switching. The aim of rotating back the angle θ_3 is to facilitate the next operation and leave space for manual switching. As shown in Fig.5, when the value for this angle θ_3 is set as half of the partial gear, the partial gear will rotates $\pi/2+\pi/2$ for the next complete connect or disconnect operation.

Under an idle load, partial gear rotation speed can be calculated as follows.

$$n_2 = \frac{24000}{419.3} = 57 \, rad / \min \tag{9}$$

$$\omega_2 = 2\pi \times n_2 = 5\pi / 6t \tag{10}$$

i.e.$t=0.42$s means the disconnect/connect operation requires 0.42 s under idle load.

4.2 Motor control procedure design

In the presented intelligent low-voltage load switch, its software of MCU should include system initialization, IO detection, motor rotation control and interrupt response modules. The system initialization module initializes the software of the MCU and hardware. The IO detection module provides the Hall sensor position, control signal, and manual/automatic mode detection. The motor rotation control module primarily controls normal motor rotation. The interrupt response module handles the internal timer interrupt, interval timer interrupt, external power disconnection interrupt and control signal interrupt. The system control procedure is shown in Fig. 6.

After the system is powered on, the main interrupt program is paused while the hardware is initialized. After hardware initialization, the main interrupt program and millisecond timer interrupt program start, and the software variables are initialized. After 4.7 s, and system startup is completed. The program detects whether a control signal is received, starts power disconnection and control signal interrupt and determines if the motor requires operation. If the motor operation is needed, the watchdog is fed, and the motor control procedure is executed. If motor operation is not needed, then the system enters a low-power consumption state.

The feedback line provides feedback between the intelligent low-voltage load switch disconnect/connect unit and the electricity meter. The intelligent low-voltage load switch disconnect/connect control unit also detects a DC motor state via the Hall sensor. Before the intelligent low-voltage load switch executes a control command, it detects a motor feedback state and electricity meter control signal. Based on the detection result, the corresponding operation procedure should be executed. The motor program control procedure is shown in Fig. 7.
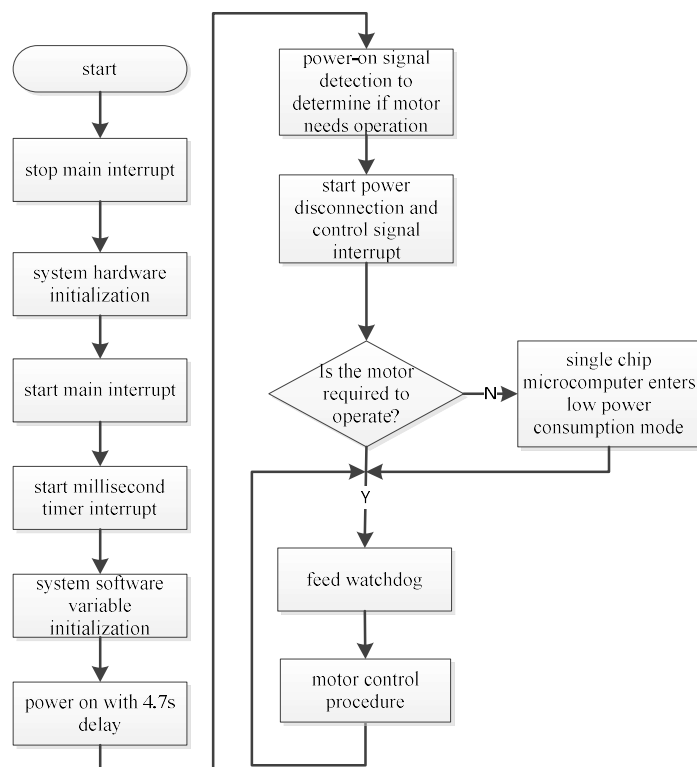
Figure.6   System control procedure

As shown in Fig. 7, the control unit detects a low-voltage load switch feedback state, electricity meter control signal and low-voltage load switch position state. When a control signal change is detected, the following procedure is executed:

(1) If the low-voltage load switch position is in the connect position, then the motor rotates backward, and the low-voltage load switch trips and operation stops.

(2) If the low-voltage load switch position is in the middle position, the electricity meter control signal is in the high level position, and the low-voltage load switch feedback state is in the disconnect position, then the control motor rotates forward to the connect low-voltage load switch.

(3) If the low-voltage load switch position is in the middle position, the electricity meter control signal is in the low level position, and the low-voltage load switch feedback state is the connect position, then the control motor rotates backward to disconnect the low-voltage load switch.

(4) If the low-voltage load switch position is in the disconnect position, then the control motor rotates forward to the connect low-voltage load switch, and operation stops.

(5) If the low-voltage load switch position is in another position and the motor state is in forward rotation, then the control motor continues forward rotation to connect the low-voltage load switch, and operation stops.

(6) If the low-voltage load switch position is in another position and the motor state is backward rotation, then the control motor continues backward rotation to disconnect the low-voltage load switch, and operation stops.

(7) If the low-voltage load switch position is in another position and the motor state is stop, then the control motor rotates backward to disconnect the low-voltage load switch, and operation stops.
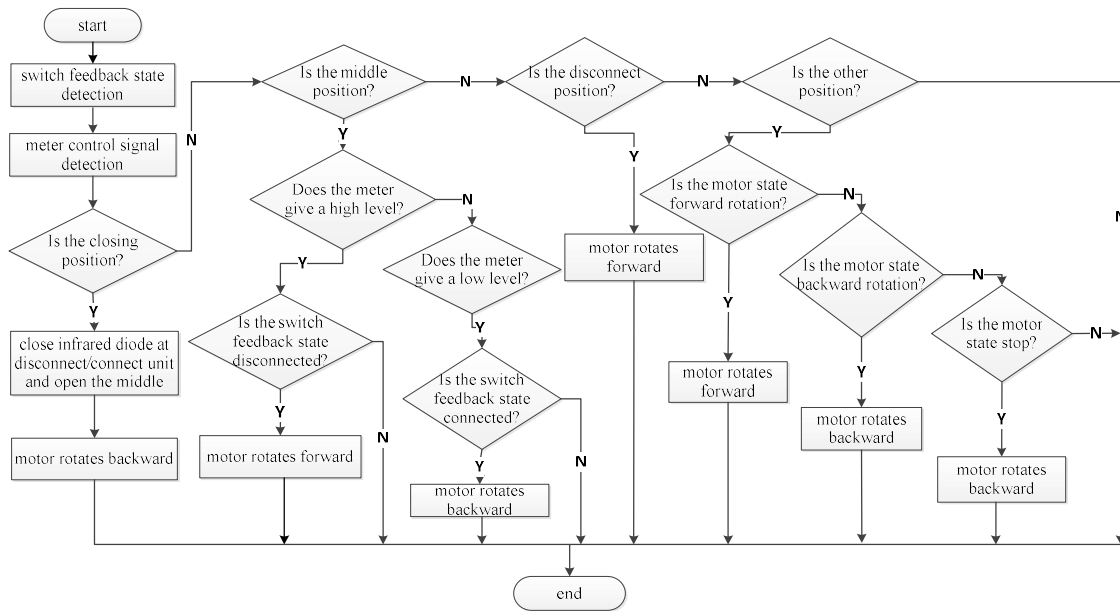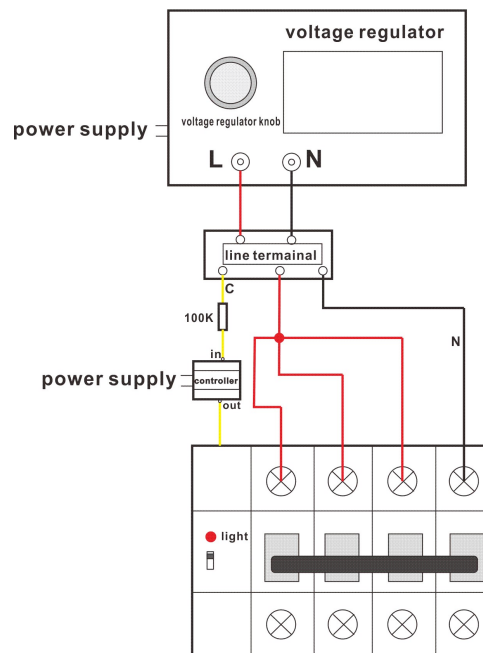
Figure.7   Motor control procedure

Figure.8   The connection between system control and feedback test

5. Function verification

5.1   Test environment setup

Voltage load switch control is based on an AC 220 V level and connected to a 100 K series resistor before providing output. When the low-voltage load switch is in a connected state, the feedback level should be AC 220 V. when the low-voltage load switch is in a disconnect state, the feedback terminal does not have a feedback signal. The system control and feedback test connection is shown in Fig. 8.
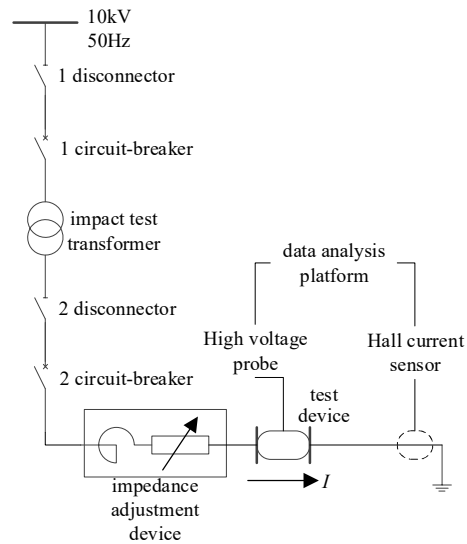
Figure 9　Test schematic

As shown in Fig.9, the test device mainly includes: impact test transformer, impedance adjustment device, high voltage probe, Hall current sensor, data analysis platform, etc. The expected short circuit current of 10kA is generated by the impact test transformer and the impedance adjustment device. The high-voltage probe detects the voltage across the sample of the external load switch, and the Hall current sensor detects the current flowing through the sample circuit. Test conditions: rated voltage U_e=230.0V on the secondary side of the transformer, expected short-circuit current I=10kA, power factor $\cos\theta$=0.95(L).

5.2　Test results

Intelligent low-voltage load switch samples are selected, and their control and feedback systems are tested in a predefined test sequence. An image of the control and feedback system is shown in Fig. 10. Switch experiment results and test waveforms are reported in Fig. 11.
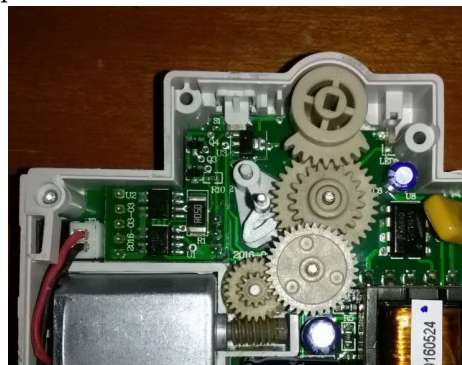

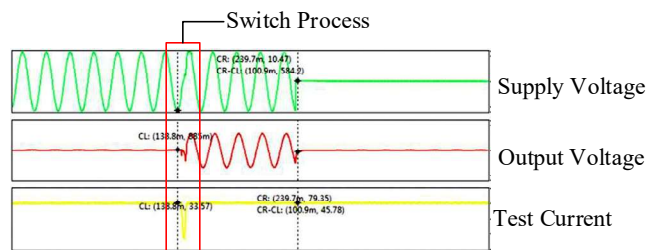Figure.10　Image of a control and feedback system

Figure.11   Switch experiment results and test waveforms

The test results of control performance and state control capability are listed in Table 2 and Table 3, respectively.

Table 2. Control performance test results

test item	test result
signal feedback method detection	control signal is AC 220 V; feedback signal is AC 220 V; phase line leak current is I_L=0.195 mA<0.2 mA; control level current is I_c=0.890 mA<1 mA; apply control level at 70%–120% of the rated voltage (220 V) for normal operation.
driving capability and AC 220 V level control test	satisfy requirement in Table 3
power-on delay test	t_d=5 s>4.5 s
remote automatic connect time	t_c=2.5 s<3 s
synchronism test	operations are essentially synchronous (difference < 7 ms)

In Tables 2, the power-on delay time t_d means that when the line power changes, the load switch should remain in its original state and do not react to changes in the received level control signal within 4s after power-up. This situation effectively prevents a signal-fluctuation-induced false operation. The remote automatic closing time t_c represents the time from when the load switch receives the level control signal to when the load switch is closed, which reflects the logic processing capability of the control circuit and the chip and the action capability of the electric part.

For the remote automatic closing time test, the AC 220V power supply is directly connected to the input terminal of the external load switch. A control switch is connected in series with the input terminal of the L line of the external load switch to the control terminal. The control terminal of the external load switch and the output terminal of the L line are connected to the power-on time tester. After turning on the control switch on the control end, the power-on time tester starts timing, and the external load switch automatically performs the closing operation. When the output terminal detects an AC 220V voltage, the power-on time tester stops timing and records the time value. Repeat the measurement 3 times, and the time value of each time should be less than 3s.

For the driving ability test, the AC154V (70% rated value), AC220V, and AC264V (120% rated value) control voltages are applied to the sample to be tested through the voltage regulator, and a 100kΩ resistor is connected in series. The voltage signal is applied to the control end of the external load switch. The external load switch should be able to operate reliably 50 times, with an interval of 10s after each action is completed. The external load switch should not be damaged after the experiment.

For the level control test, the external load switch of the energy meter adopts AC 220V as the control level. In order to play a role in current limiting and protection, a 100kΩ resistor must be connected in series in the control and feedback lines. When the external load switch is closed, the feedback level signal is AC 220V; when the external load switch is open, the feedback terminal has no feedback signal (the line is in the open state).

As shown in Tables 2 and 3, the result of t_d and t_c are 5 s and 2.5 s, respectively. When the line power supply changes and the control signal changes, the control logic of the intelligent low-voltage load switch meets the requirements of enterprise standard of State Grid Corporation of China (Q/GDW11421-2015) "Technical Specifications for External Circuit Breakers of Electric Energy Meters" [29], and a complete set of fee control functions is realized.

Table 3. State control capability test results

phase line	control signal line	initial state	completion state	test result
AC 220 V	↑	disconnect	connect	(from 0 V to 220 V) connect signal received
AC 220 V	↓	connect	disconnect	(from AC220 V to 0 V) disconnect signal received
AC 220 V→0 V →AC 220 V	AC 220 V	connect	connect	connected before line disconnection, connected again after line disconnection
AC 220 V→0 V→AC 220 V	0 V	disconnect	disconnect	disconnected before line disconnection, connected again after line disconnection
0 V	/	disconnect	disconnect	line disconnected, maintain original state
0 V	/	connect	connect	line disconnected, maintain original state

Moreover, experiments also have been carried out to investigate the output voltage and test current for suppressing arc in the designed switch. Results are reported in Table.4.

Table 4   Result of arc extinguishing test during switch breaking process

Samples	Voltage/V	Current/A	Arcing time/ms	Breaking time/ms
1	205.5	2632.6	6.4	9.1
2	201.6	2745.9	6.2	8.9
3	203.8	2643.7	6.9	9.7
4	216.7	2758.4	4.6	8.3
5	210.4	2752.3	4.3	8.1
6	211.1	2742.4	4.7	8.5

In Table 4, test samples 1-3 are the state-of-art switches, while samples 4-6 are the proposed intelligent low-voltage load switches. From Table 4, it can be seen that the breaking time and arcing time of the proposed intelligent low-voltage load switches are generally reduced than those of the state-of-art switches. Moreover, compared with the state-of-art switches, the effective value of the voltage of the proposed intelligent low-voltage load switches increases, closer to 220V, while the effective value of the current does not change significantly during the breaking process.

The test results indicate that when the line power supply and control signal change, the control logic of this intelligent low-voltage load switch satisfies the enterprise standard of State Grid Corporation of China (Q/GDW11421-2015) "Technical Specifications for External Circuit Breakers of Electric Energy Meters" [29] and provides a complete payment control function.

Conclusions

To address the challenge that current implementations of low-voltage load switch do not support remote disconnect/connect and accurate feedback of a disconnect/connect state, this paper presents an intelligent low-voltage load switch with remote control and real-time monitoring of state. The test results indicate that this system design is practical, feasible and supports disconnect/connect control and state feedback in various conditions and satisfies the requirements of the enterprise standard of State Grid Corporation of China (Q/GDW11421-2015). This design solves the disadvantage that a current low-voltage load switch does not support remote disconnect/connect and real-time monitoring of a switch state. The design has high practical value and is worthy of promotion.

References

1. T. Chmielewski, P. Oramus, M. Szewczyk, T. Kuczek, W. Piasecki, Circuit breaker models for simulations of short-circuit current breaking and slow-front overvoltages in HV systems [J].Electric Power Systems Research, 2016, 143(10): 174-181.

2. J.Aronstein and R.Lowry, Estimating fire losses associated with circuit breaker malfunction [J]. IEEE Trans. Ind. Appl., 2012, 48(1): 45-51.

3. C.Franck, HVDC circuit breakers: A review identifying future research needs [J].IEEE Trans. Power Del., 2011, 26(2): 998-1007.

4. Qi, Zhe, Zhu, Zhi Hong, Xu, Wei. Electro-optic switching based on a waveguide-ring resonator made of dielectric-loaded graphene plasmon waveguides [J]. Journal Of Power Electronics, 2016, 16(5): 1639-1649.

5. Jiang Ya-zhou, Liu Chen-Ching, Diedesch, Michael. Outage Management of Distribution Systems Incorporating Information From Smart Meters [J]. IEEE Transactions On Power Systems, 2016, 31(5): 4144-4154.

6. Hanson, Reed, Reitz, Rolf. Investigation of Cold Starting and Combustion Mode Switching as Methods to Improve Low Load RCCI Operation [J]. Journal Of Engineering For Gas Turbines And Power-Transactions Of The Asme, 2016, 138(9): 117-120.

7. Diaz, Guzman, Morreno, Blanca. Valuation under uncertain energy prices and load demands of micro-CHP plants supplemented by optimally switched thermal energy storage [J]. Applied Energy, 2016, 177(9): 553-569.

8. Chen Qipeng, Kaleshi, Dritan, Fan, Zhong. Impact of Smart Metering Data Aggregation on Distribution System State Estimation [J]. IEEE Transactions On Industrial Informatics, 2016, 12(4): 1426-1437.

9. Sun, Qie, Li, Hailong, Ma, Zhanyu. A Comprehensive Review of Smart Energy Meters in Intelligent Energy Networks [J]. IEEE Internet Of Things Journal, 2016, 4(3): 464-479.

10. Islam, Asif, Birtwhistle, David, Saha, Tapan Kumar. Two-Part Synthetic Test Procedures for the Testing of Medium-Voltage Load Break Switches [J]. IEEE Transactions On Power Delivery, 2016, 107(4): 804-817.

11. Hwang, Kwang-il, Jeong, Young-sik, Lee, Deok Gyu. Hierarchical multichannel-based integrated smart metering infrastructure [J]. Journal Of Supercomputing, 2016, 72(7): 2453-2470.

12. Ramaiaha Ananthapadmanabha Berigai,Maurya Rakesh,Arya Sabha Raj,Magnetic energy recovery switch-based power quality AC-DC converters [J]. International transactions on electrical energy systems, 2017, 27(8): 1-16.

13. Dezhi Xiong, Xiangqun Chen, Jie Yang. Optimization of a Low-Voltage Load Switch for a Smart Meter Based on a Double Response Surface Model[J]. MAPAN-Journal of Metrology Society of India, 2018, 3(33), 261-270.

14. Dezhi Xiong, Xiangqun Chen, Jie Yang, Yi Zuo. Arcing failure analysis of miniature circuit breaker using nano-W–Cu material[J]. Emerging Materials Research, 2018, 7(1), 25-31.

15. J. Zhang, H. Wen, and L. Tang, "Improved Smoothing Frequency Shifting and Filtering Algorithm for Harmonic Analysis With Systematic Error Compensation," IEEE Transactions on Industrial Electronics, vol. 66, pp. 9500-9509, 2019.

16. J. Zhang, L. Tang, A. Mingotti, L. Peretto, and H. Wen, "Analysis of White Noise on Power Frequency Estimation by DFT-based Frequency Shifting and Filtering Algorithm," IEEE Transactions on Instrumentation and Measurement, Early Access，2019, DOI: 10.1109/TIM.2019.2941290.

17. H. Wen, C. Li, and W. Yao, "Power System Frequency Estimation of Sine-Wave Corrupted With Noise by Windowed Three-Point Interpolated DFT," IEEE Transactions on Smart Grid, vol. 9, pp. 5163-5172, 2018.

18. He Wen, Junhao Zhang, Zhuo Meng, Siyu Guo, Fuhai Li, Yuxiang Yang. "Harmonic Estimation Using Symmetrical Interpolation FFT Based On Triangular Self-Convolution Window". IEEE Transactions on Industrial Informatics, 11(1):16-26, 2015.

19. Stratil, T., Koudelka, P., Martinek, R., & Novak, T. (2017). Active pre-equalizer for broadband over visible light. Advances in Electrical and Electronic Engineering, 15(3), 553-560.

20. Hekmatmanesh, A., Mikaeili, M., Sadeghniiat-Haghighi, K., Wu, H., Handroos, H., Martinek, R., & Nazeran, H. (2017). Sleep spindle detection and prediction using a mixture of time series and chaotic features. Advances in Electrical and Electronic Engineering, 15(3), 435-447.

21. Kahankova, R., Jezewski, J., Nedoma, J., Jezewski, M., Fajkus, M., Kawala-Janik, A., Martinek, R. (2017). The influence of gestation age on the performance of adaptive algorithms used for fetal ecg signal extraction. Advances in Electrical and Electronic Engineering, 15(3), 491-501.

22. Nedoma, J., Fajkus, M., Kepak, S., Cubik, J., Kahankova, R., Janku, P., Martinek, R. (2017). Noninvasive fetal heart rate monitoring: Validation of phonocardiography-based fiber-optic sensing and adaptive filtering using the nlms algorithm. Advances in Electrical and Electronic Engineering, 15(3), 544-552.

23. Khankova, R., Jaros, R., Martinek, R., Jezewski, J., Wen, H., Jezewski, M., & Kawala-Janik, A. (2017). Non-adaptive methods of fetal ecg signal processing. Advances in Electrical and Electronic Engineering, 15(3), 476-490.

24. Nedoma, J., Fajkus, M., Siska, P., Martinek, R., & Vasinek, V. (2017). Non-invasive fiber optic probe encapsulated into PolyDiMethylSiloxane for measuring respiratory and heart rate of the human body. Advances in Electrical and Electronic Engineering, 15(1), 93-100.

25. Nedoma, J., Fajkus, M., Martinek, R., & Vasinek, V. (2017). Non-invasive fiber-optic biomedical sensor for basic vital sign monitoring. Advances in Electrical and Electronic Engineering, 15(2), 336-342.

26. Martinek, R., & Zidek, J. (2012). The real implementation of NLMS channel equalizer into the system of software defined radio. Advances in Electrical and Electronic Engineering, 10(5), 330-336.

27. Datasheet of Hall sensor OH137. https://www.alldatasheet.com/view.jsp?Searchword=OH137

28. Datasheet of R5F10268 chip. https://www.renesas.com/sg/en/doc/products/mpumcu/doc/rl78/r01ds0193ej0210_rl78g12.pdf

29. Q/GDW11421-2015, "Technical Specifications for External Circuit Breakers of Electric Energy Meters", The enterprise standard of State Grid Corporation of China.

Conflicts of Interest: The authors declare no conflict of interest

Availability of data and material (data transparency): Not applicable

Code availability (software application or custom code) : Not applicable

Author Contributions: conceptualization, Dezhi Xiong and He Wen; validation, Dezhi Xiong and Xiangqun Chen; formal analysis, Dezhi Xiong and Derong Luo; writing—original draft preparation, Dezhi Xiong and He Wen; writing—review and editing, Radek Martinek and Janusz Smulko; supervision, He Wen; project administration, Xiangqun Chen, He Wen and Derong Luo.